



Preparation and Annealing Effects on the Structural and Optical Properties of ZnTe Thin Film

Zainab Assif Abdullah¹  , and Ayad Ahmed Salih^{2*}  

¹University of Technology, Baghdad, Iraq

²Department of Physics, College of Education for Pure Science (Ibn Al-Haitham), University of Baghdad, Baghdad, Iraq

*Corresponding Author

Received: 8/July/2025

Accepted: 4/December/2025

Published: 20/April/2026

doi.org/10.30526/39.2.4227



© 2026. The Author(s). Published by College of Education for Pure Science (Ibn Al-Haitham), University of Baghdad. This is an open-access article distributed under the terms of the [Creative Commons Attribution 4.0 International License](https://creativecommons.org/licenses/by/4.0/)

Abstract

ZnTe possesses the proper optoelectronic properties as a candidate for device development. The structure and optical properties of ZnTe semiconductor thin films of 500 nm were studied using thermal evaporation technique. The influence of annealing temperatures on ZnTe thin films in the range (R.T - 473 K). XRD and surface morphological analyses are used to examine the films. The ZnTe films are comparatively polycrystalline and cubic in phase, according to the XRD analysis. with a lattice constant of 0.61 nm upon an (111) orientation. The intensities of all the peaks rapidly increase though they show the same tendencies; it shows the crystallinity of the films becomes higher crystal size diameters (from 8.41 to 12.18nm) both increase as the temperature of annealing increases. The transmittance data within the wavelength range of 400–1000 nm was employed to calculate the optical absorption coefficient (α) of the films. We have calculated the real and imaginary parts of the dielectric constant, the extinction coefficient, and the refractive index as a function of wavelength, and our results demonstrate that the optical energy band gap of telried zinc The thin film drops from 2.15 eV to 2.02 eV as the annealing temperature rises.

Keywords: Chalcogenide semiconductors, X- ray diffraction (XRD), Atomic Force Microscopy (AFM), Band gaps ZnTe, Thin film.

1.Introduction

In the present study, ZnTe thin films are prepared by vacuum evaporation and the impact of annealing at (373, 473) K on them is investigated with respect to their optical properties, XRD, AFM, and the correlation of these parameters. ZnTe is a chalcogenide semiconductor substance belonging to the II–IV transition group¹. It was generally determined to be of P-type and have an energy gap of (2–2.3) eV and that it has high conductivity and solar cell efficiency². Due to this band gap, such is a pure green region of the electromagnetic spectrum and for such reason it is important to develop pure green lamps of LED. It has also been experimentally demonstrated that the (ZnTe) has a high photoelectric coefficient which is useful for generation of terahertz (THz) radiation and detecting the same³. Zinc telluride has important electrical and optical properties for semiconductor applications. It has been used to made many kind of optical instruments. It is lattice constant is (0.6101) nm and has gray or brownish powder or ruby red color or a ruby red crystal. To create thin films of ZnTe, a variety of methods have been tried, such as sputtering, electron beam evaporation, metal-organic chemical vapor deposition (MOCVD), electron beam growth to form thin films of (ZnTe) and thermal evaporation⁴⁻⁷. This work emphasizes how temperature affects structural and optical properties. The compound ZnTe is an extremely important material since it is utilized in production of various optoelectronic

devices, such as lasers, light-emitting diodes, and solar cells^{8, 9}. The process of creating thin films (ZnTe) utilizing the evaporation method of deposition is also very important due to its several applications including use for the window layer of any electronic device^{10,11} and electronic and optical devices such as a low wavelength photodetector^{6, 12, 13}. The optical and compositional observation of the thin film implies that it holds promise for the production of LEDs., detectors and solar cells^{7, 14,15}.

2. Materials and Methods

ZnTe alloy has been prepared. The high purity (99.999 %) of Zinc (Zn) and telluride (Te) elements (from Sigma-Aldrich USA Company) were pre-hand mixed with 1:1 stoichiometric weight using high purity metals. The product alloy placed into quartz tubes was pressurized with 1×10^3 mbar, before being heat treated for 6 hours in an electric oven at 1273 K, where it should be mentioned that the temperature needed for complete alloy solidification was above the ZnTe melting temperature, according to the phase diagram¹⁶. The substance was applied to glass substrates at a rate of 4.5×10^{-5} Torr to create a layer that was around 500 nm thick by using the weight method for measuring thin film thickness.

The glass substrate surface needs to be completely cleaned to get rid of any contaminants in order to produce a homogeneous thin film semiconductor with good adhesion. The structure (morphology) of ZnTe has been ascertained using X-ray diffraction (XRD) and AFM. Following an analysis of these films' X-ray diffraction, the crystallite size was calculated using Scherer's Formula depending on the film thickness¹⁷:

$$C.S = \frac{0.9 \lambda}{\beta \cos(\theta)} \quad (1)$$

The diffraction width of the peaks at half maximum is denoted by the symbol β (FWHM). (C.S) is the crystallite size and (θ) the diffraction peak angle. Determination of lattice constant (a) is done by below equation¹⁸:

$$\frac{1}{d^2} = \frac{h^2 + k^2 + l^2}{a^2} \quad (2)$$

Where Miller incidents (hkl). The calculation of (ϵ) micro strain for manufactured thin film can be determined using the following¹⁹:

$$\epsilon = \frac{\beta \cos \theta}{4} \quad (3)$$

The density of dislocations (δ) is the ratio of the lengths of the dislocation line to the crystal volume. It may be calculated using the following²⁰:

$$\delta = \frac{1}{(C.S)^2} \quad (4)$$

To determine the energy gap, Measurements of optical transmission within the wavelength range of 400-1000 nm were performed. Optical characteristics of the thin film preparation have been observed through transmission and absorption spectra spanning a wavelength range of 400 to 1000 nanometers. The Lambert law and Tauc equations have been used to calculate the energy gap (E_g) from the absorption spectra, respectively¹⁸:

$$\alpha = 2.303 \frac{A}{t} \quad (5)$$

$$\alpha h\nu = D (h\nu - E_g)^r \quad (6)$$

the exact value of the temperature-dependent variable D. The symbol α refers to the absorption coefficient, the energy magnitude of the incident photons is indicated by $h\nu$, and the optical transition type is specified by (r). Thickness (t) and absorption (A).

The dielectric constant's extinction coefficient (k), refractive index (n), real part (ϵ_r), and imaginary part (ϵ_i), and the reflection(R) are among the relationships that can be utilized to compute optical constants²¹:

$$k = \frac{\alpha \lambda}{4\pi} \quad (7)$$

$$n = \left[\frac{4R}{(1-R)^2} - k^2 \right]^{1/2} + \frac{(1+R)}{(1-R)} \quad (8)$$

$$\varepsilon_r = n^2 - k^2 \quad (9)$$

$$\varepsilon_i = 2nk \quad (10)$$

3.Results

X-ray diffraction (XRD) was employed to detect the effect of annealing temperatures (R.T, 373 and 473) K on the crystallization behavior of the investigated ZnTe thin films. In this study investigated X-Ray Diffraction for alloy prepared and the deposition thin films, the scanning angle 2θ was varied in the range of 10° - 80° . Annealing effect has been examined by X-ray diffractions using (SHIMADZU-Japan-XRD 6000) diffractometer system which records the intensity as a function of Bragg's angle as show in **Figure 1**, also the dislocation density (δ) and the micro strain (ε) were decreases with increasing the annealing temperatures.

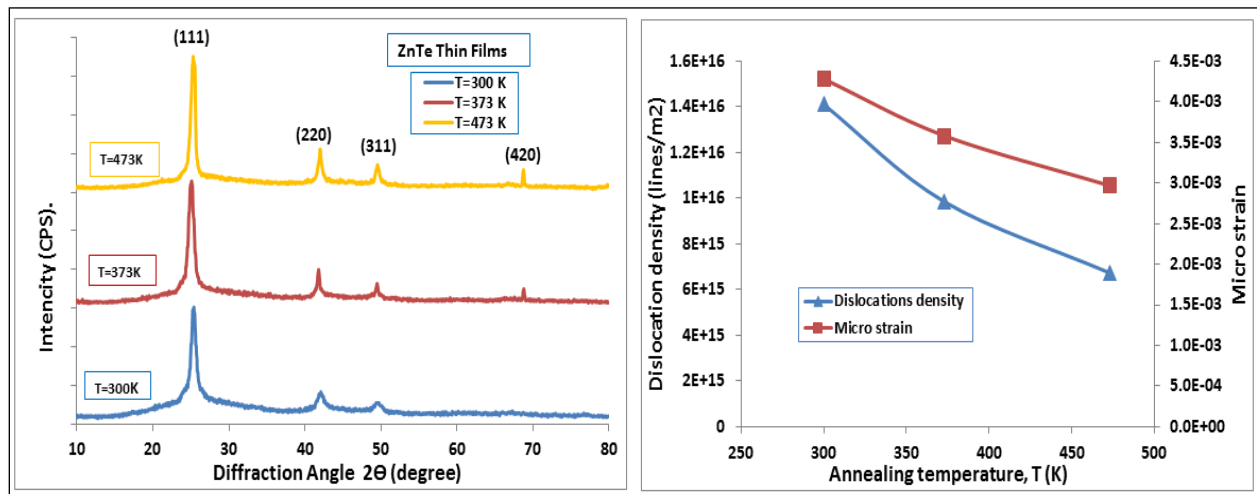


Figure 1. X-ray diffraction for the ZnTe thin films (R.T K, 373 K and 473 K)

The general structure of ZnTe alloy and annealing thin films, including inter planer distance $d(hkl)$ for different planes, lattice constants, crystallite size (C.S), the dislocation density (δ), and the micro strain (ε) are determined and compared with value in the Joint Committee on Powder Diffraction Standard (JCPDS) cards for ZnTe as shown in **Table 1**.

Table 1. X-ray diffraction data for ZnTe thin films at various annealing T. (R.T, 373 and 473)K.

T_a (K)	$d_{exp.}$ (Å)	$2\theta_{exp}$ (deg)	(hkl)	FWHM (deg)	C.S (nm.)	$\delta \times 10^{15}$ (lines/m ²)	$\varepsilon \times 10^{-3}$
R.T	3.5222	25.26	(111)	0.98	8.64	13.37	4.18
	2.1494	42.00	(220)				
	1.8371	49.58	(311)				
373	3.5239	25.25	(111)	0.82	10.34	9.35	3.50
	2.1583	41.82	(220)				
	1.8402	49.49	(311)				
	1.3634	68.80	(420)				
473	3.5265	25.23	(111)	0.68	12.49	6.41	2.89
	2.1504	41.98	(220)				
	1.8385	49.54	(311)				
	1.3644	68.74	(420)				

It was used atomic force microscope (AFM) to study the effect of annealing temperatures (R.T, 373, and 473) K on mapping topography surfaces of the thin films. The study was recorded by

using scanning probe microscope (type AA3000, supplied by Angstrom Advanced Inc. USA), for three-dimensional images describing the surface in terms of roughness and grain size, and these images of high precision values as shown in **Figure 2**.

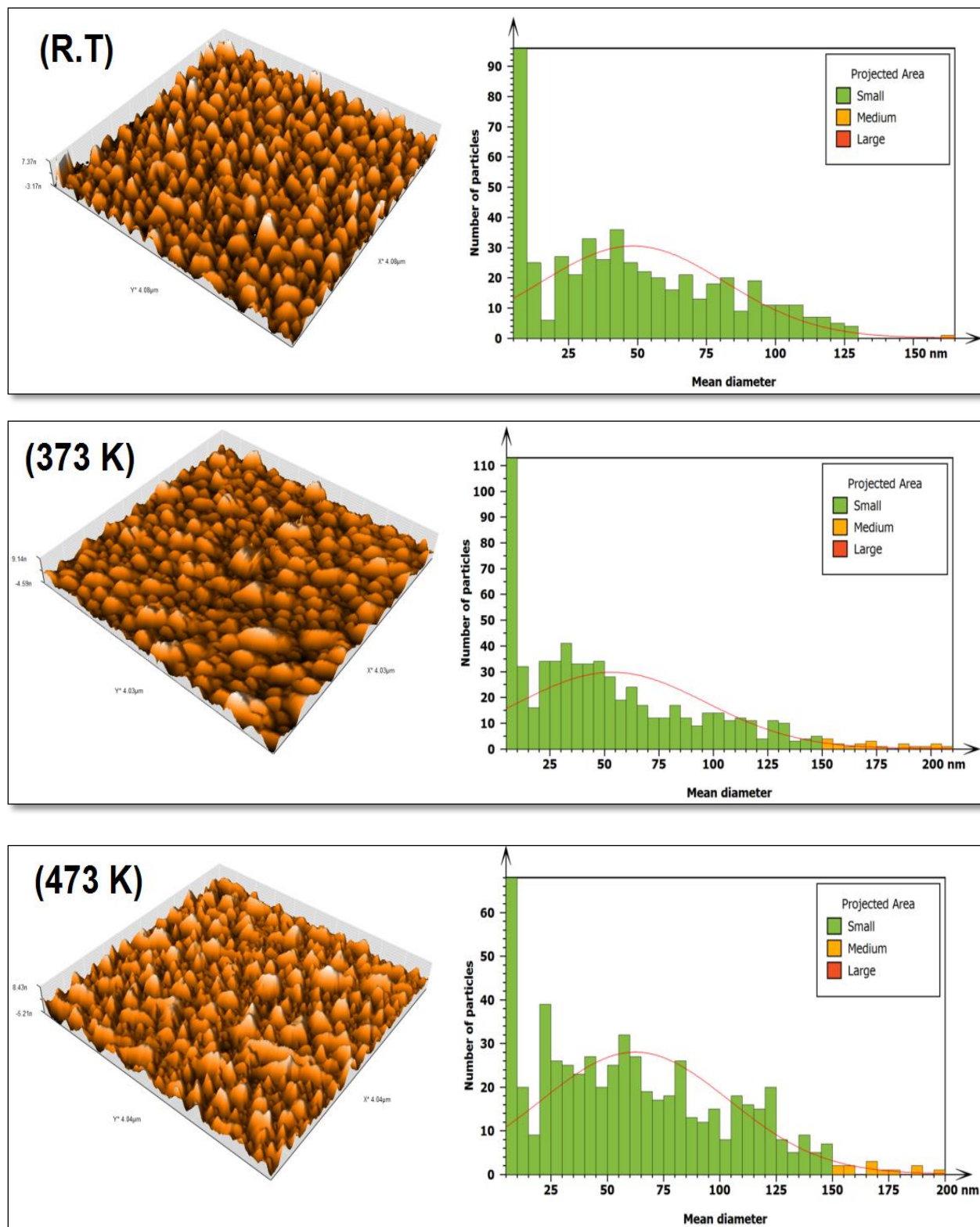


Figure 2. AFM image for the ZnTe thin films at (R.T K, 373 K and 473 K).

From **Figure 2** and **Table 2**, it can be observed that the films are found to be uniform and densely packed without any cracks or pinholes and the average grain size was increased as the

annealing temperature increase, and the roughness of the surface was increases too, this may be due to aggregation of grains into the larger clusters and also growth of some crystal planes

Table 2. Average roughness, grain size, and ZnTe thin films' root mean square at (R.T, 373, and 473) K.

Thickness (500 nm)	Grain size (nm)	Surfaces roughness (nm)	Root mean square (nm)
R.T	48.36	2.954	3.628
373	53.59	3.980	5.558
473	62.39	6.375	7.929

Optical measurement constitutes the most important means of determining the band structure of semiconductors. Where the optical properties of ZnTe thin films deposited on glass slide which include the transmittance and absorbance spectra were studied over the wavelength range (400-1100) nm by using UV-Visible 1800 Spectra Photometer as shown in **Figure 3**.

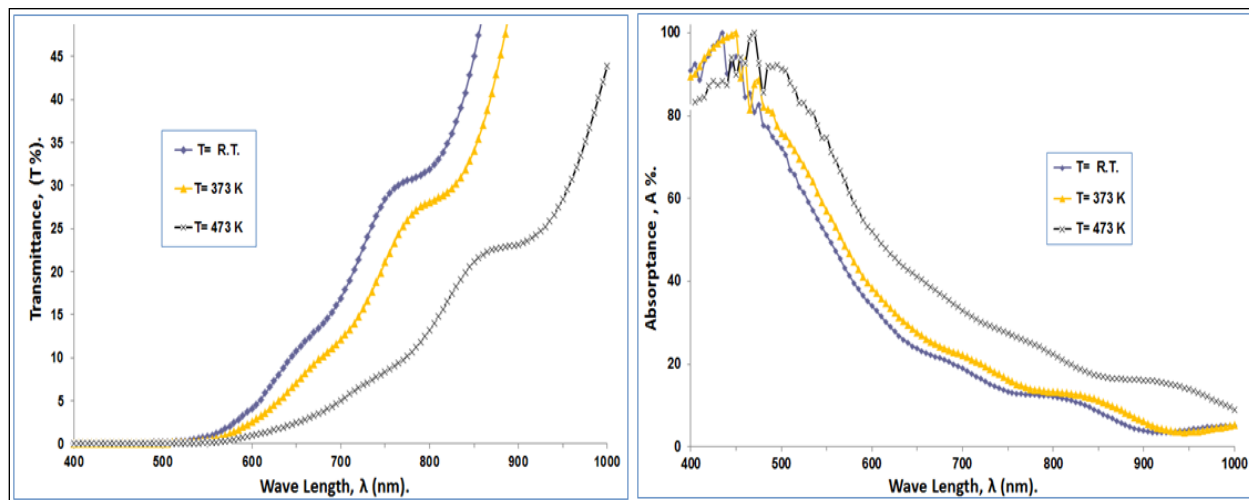


Figure 3. Transmittance and absorption spectrum of ZnTe at (R.T, 373 and 473) K

Optical absorbance data were used to calculate the transmittance, absorption coefficient (α), band gap energy (E_g) as shown in **Figure 4** and the optical constants {extinction coefficient (k), refractive index (n), and real and imaginary parts of dielectric constant} for ZnTe thin films with annealing temperatures (R.T, 373 and 473) K deposited with thickness of 500 nm on glass slides substrate as shown in **Figure 5**.

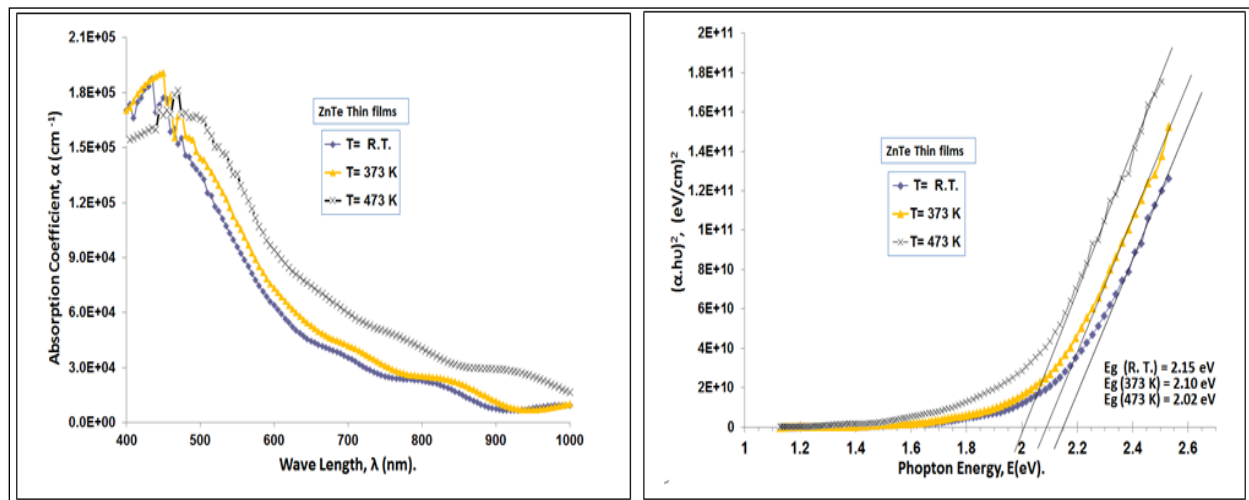


Figure 4. Variation in the optical constants (Refractive index n , Extinction coefficient k , Dielectric constants (real and imaginary) with wavelength for ZnTe at temperature (R.T, 373 and 473)

Table 3 shows the evaluated some of the optical constants values (gap energy E_g , absorption coefficient α , refractive index n , extinction coefficient k , real and imaginary parts of dielectric constant) at different annealing temperatures in the visible light range ($\lambda = 550$ nm)

Table 3. Optical parameters of (E_g^{opt} , α , n , k , ϵ_r & ϵ_i) ZnTe at (R.T, 373, and 473) K with $\lambda = 550$ nm..

Thickness (500 nm)	E_g^{opt} (eV)	$\alpha \times 10^4$ (cm ⁻¹)	n	k	ϵ_r	ϵ_i
R.T	2.15	9.59	5.48	0.42	29.94	4.61
373	2.10	10.89	4.69	0.47	21.79	4.47
473	2.02	13.55	2.86	0.59	7.88	3.40

Optical constants included refractive index (n), extinction coefficient (k), real part (ϵ_r) and imaginary parts (ϵ_i) of optical dielectric constant. It is obvious from **Figure 5** effect of annealing temperatures, the refractive index values increase while the extinction coefficient decreases with the increase photon energy, than at higher photon energy the refractive index values decreases reaching the lowest value with increase annealing temperatures.

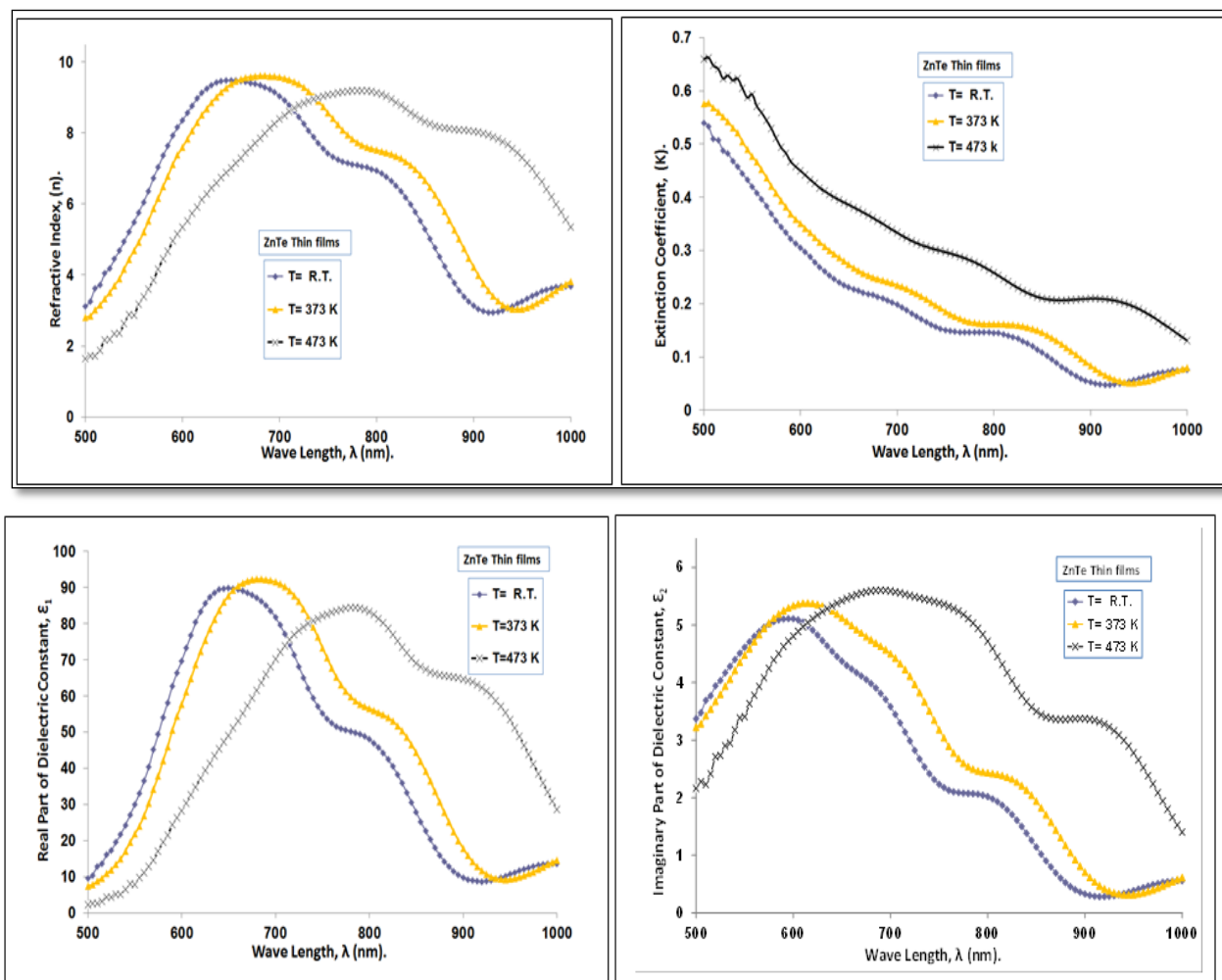


Figure 5. Variation of The optical parameters (n , k , ϵ_1 , ϵ_2) versus wavelength for ZnTe at temperature (R.T, 373 and 473) K.

4. Discussion

The room temperature and (373, 473) K. XRD spectra of 500 nm thick of the ZnTe thin films displays the annealed and not annealed films as given in the **Figure 1**. The polycrystalline nature of the ZnTe film compound in cubic structure is seen in the multi-diffraction peaks of the (111), (220), (311) and (420) planes. With the JCPDS file number 00-015-0746 card standard value, the XRD peaks match the crystal's cubic structure. In addition, the films show the preferred growth direction to be in accordance with plane (111). Each diffraction peak can be assigned to binary

compound ZnTe, JCPDS file. Annealing of the films at 373 and 473 K showed no shift in the diffraction peak positions but increased the peak intensity and the crystallite size (C.S.), which indicating improved crystallinity of the film, the defects were reduced and the regularity in the crystal structure was increased. The film's crystallite size seen in **Figure 1** can be determined using the Scherrer equation, which relies on the FWHM of the (111) peak. As seen by the data in **Table 1**, the crystallite size grows as the ZnTe annealing temperature rises. The lattice constants value $a = 6.1007 \text{ \AA}$ are in good agreement with the same of research ^{1,10}. As indicated in **Table 1**, the standard "d" and "a" values derived from JCPDS are in good agreement with the observed "d" and "a" values. Such strong crystallinity with $T_a = 473 \text{ K}$ in ZnTe thin_films has a significant impact on their electrical, optical, and thermoelectric characteristics. The uniform, flat surfaces of the films are crucial for their applications in different technical devices, such as thermoelectric generators, photodetectors and solar cells

The micro strain (ϵ) and dislocation density (δ) have been already calculated and as displayed in **Table 1**. As the annealing temperature rises, it is noticed that the dislocation density and micro strain decrease in the visible range. The behavior can be interpreted by the negative correlation of dislocation density and crystallite size and the positive correlation of micro strain and full width at half maximum (FWHM) of the dominant peak. The decrease in defects of ZnTe thin film samples on with increasing annealing temperature opens up the possibility to improve the crystal structure. The change of the morphology of the films was investigated by the AFM scan of surface morphology. Thin film micro-roughness is an important criterion for optical coatings, especially in the UV range for application such as heat mirrors and lithography ²⁰. The RMS roughness not only reflects the light scattering but also sheds light on the quality of the surface being examined. The AFM images of ZnTe thin films with temperatures at R.T, 373 K and 473 K are presented in **Figure 2**. The images above show that the movie is evenly dispersed and clear of islands and pinholes. and also has a high density of columnar grains. The morphological features of the structure i.e., roughness height, root mean square, and average diameter (G.S) are shown in **Table 2**. Average grain size varied between structures (48.36-62.39 nm), and the roughness and root mean square values also showed variations. The annealing thin film data are then summarized in This table shows the increase in root mean square, roughness, and average grain size. For this reason, the films' increased surface roughness suggests that they might be used as anti-reflective coatings, which would increase light absorption and decrease light reflection in the visible portion of the spectrum²⁰. At 473 K, sample ZnTe also shows a main magnitude. This can be attributed to the increased atomic mobility that leads to the particle aggregation, especially to the bigger particles. The XRD analysis above and the AFM observation results correlate well. The Using a UV/Visible (1800) spectrophotometer, optical transmission was measured. The transparent films' optical transmission spectra were used to determine their band gap (E_g). The relation of making the transmission curve (nm) as function of the wavelength is depicted over the wavelength, as shown in **Figure 3**, enables us to find traces of the absorbance and the transmission in the range (400–1000) nm. This indicates that ZnTe thin films at R.T. and (373,473) K have a high absorption of about 85% in the visible spectrum regions.

With increasing annealing temperature, we find the transmittance is reduced, although the absorbance and deflection are enhanced, in agreement with the fact that a band tail form the fundamental absorption edge to long wavelength (low energy). This occurrence could be explained by the way The connection between surface shape and absorbance rise is ascertained by atomic force microscopy (AFM) and X-ray diffraction (XRD) ^{19, 22}. data the thin films have been observed to exhibit increasing values of absorbance after the post-annealing process. The explanation of this increase is the absorption of photons by free carriers. Therefore, transmittance is lowered. Alternatively, it might be related to the Crystallite size growth ^{4, 18, 24} Thus, the absorption of low energy photons may occur. The absorption edge shifts toward longer wavelengths as the annealing temperature increases, suggesting that higher annealing

temperatures lead to a reduction in the band gap, hence the band gap's decrease with rising temperatures. The photon and band gap energies have a significant impact on the absorption coefficient, indicating how well a material absorbs light^{3, 25}. **Figure 4** displays the optical absorption coefficient as a function of photon energy for varying annealing temperatures. However, using the transmittance spectrum, one can also use **Equation (5)** to calculate a thin film's absorption coefficient (α) given its thickness (t). Calculated herein values of the absorption coefficients are in the interval 10^5 cm^{-1} . **Figure 4** demonstrates that the absorption coefficient (α) reaches high values at higher photon energies, suggesting a high probability of allowed direct transitions. As the wavelength increases, α gradually decreases. Additionally, the results indicate that absorbance increases with higher annealing temperatures, with a notable increase seen close to the band gap edge, and this agrees with the research^{5, 26}. Consequently, the absorption edge shifted in the direction of the long wavelength region. This disparity could be related to the effects of the annealing temperature on the carrier concentration and crystallinity of the ZnTe film. **Equation (6)** is used to get the ZnTe films' optical band gap. The permitted direct ($r = 1/2$) is specified by the parameter (r), an index associated with the material's nature that is established by the optical transition involved in the absorption process. The energy of the optical band gap. Following **Figure 4** shows the extrapolation of the straight-line portion of the $(\alpha h\nu)^2$ versus $(h\nu)$ plot curve. E_g was computed using the intercept on the photon energy axis. The transition was directly allowed of ZnTe film was calculated from 2.15 eV to 2.02 eV and fill in **Table 3** with strong agreements with^{4, 24}. Therefore, We came to the conclusion that all ZnTe thin films belong to the direct band gap material class. One crucial feature for photovoltaic applications is the film's direct band transitions. When electromagnetic radiation hits a film surface, part of it is absorbed, some is reflected, and some is transmitted. The optical behavior of materials is fully described by the optical constants, which are important fundamental properties of matter^{18, 27}. Optical constants included the refractive index (n) and the real and imaginary components (ϵ_1), (ϵ_2) of the dielectric constant and extinction coefficient (k). **Equation (7)** was used to calculate the extinction coefficient k based on the absorption coefficients α that were found. The extinction coefficient's fluctuation with wave length is displayed in **Figure 5**. It indicates the quantity of energy absorbed by the thin films and is the degree of attenuation in the electromagnetic radiation intensity. At annealing temperatures, we observe that the extinction coefficient gradually increases as photon energy rises^{19, 28}, followed by a sharp rise in high photon energies. This suggests that absorption is increasing, which in turn causes the absorption coefficient to rise. We see that the curves typically exhibit the same behavior as previously mentioned, with the absorption edge moving towards low photon energies. This confirms that the annealing temperatures have a clear effect to increase the extinction coefficient¹⁹. Also, it is demonstrated that because to the structural alterations in the films, k changes significantly with annealing temperature prior to the E_g values of the films. The change in refractive index as a function of ZnTe film wavelengths at (R.T., 373, and 473) K is shown in **Figure 5**. The refractive index dispersion is essential to the research of optical materials since it plays a major role in optical communication and the design of devices for spectrum dispersion.^{18, 29}. The films' refractive index values were determined by applying **Equation (8)**. The nature of reflection is quite similar to the refractive index curve. **Table 3** displays the refractive index value for each film with a constant wavelength of 550 nm (within the visible range) based on the relationship between reflexive index and reflection. The decrease in corresponding reflection brought on by structural and compositional changes that take place throughout the annealing process is responsible for the decline in refractive index values. Furthermore, **Figure 5** shows that all of the films show anomalous dispersion since the refractive index drops when the The energy of incoming photons exceeds the E_g value. We note that with increasing annealing temperature, the refractive index decreases within the visible light region of (400-700) nm. Metals' free electrons and semiconductors' free carriers both absorb light and perform dielectric functions^{21, 30}. And the fundamental electron excitation spectrum of the films was represented by a frequency dependent

of the complex electronic dielectric constant (ϵ), which is given by the relation ($\epsilon = \epsilon_r - i\epsilon_i$), where the relationship between the real (ϵ_r) and imaginary (ϵ_i) components of the dielectric constants is influenced by the values of (n) and (k) as shown in the **Equation (9)** and **Equation (10)**, **Figure 5** illustrates how the real dielectric constant (ϵ_r) behaves almost like the equivalent refractive index (n), which is evident from **Equation (9)** due to its small value of (k). The figure also shows that in films in the visible range, ϵ_r decreases as annealing temperature increases, whereas in the NIR region, it increases with temperature. Additionally, as the annealing temperature increased, the peaks of (ϵ_r) shifted to the higher wave length (lower photon energy). As shown in **Figure 5**, the behavior of (ϵ_i) with photon energy is almost identical to that of the corresponding extinction coefficient (k). The extinction coefficient values, which are connected to the change of the absorption coefficient, are the primary determinant of (ϵ_i). The (ϵ_i) peaks for all films move to the lower photon energy as the annealing temperature rises. The values of (ϵ_r) and (ϵ_i) decreases at a wavelength of 550 nm because of the similar behavior between (ϵ_r) and (n); the behavior of (ϵ_i) is mostly reliant on the value of (k) and closely matches curves that of (k). A minor dielectric loss is indicated by the fact that the thin film at (R.T.) has a greater value than ϵ_i . The optimal optical temperatures were observed at an annealing temperature of 473 K. Finally, we can observe that both figures suggest that the values of (ϵ_r) are greater than those of (ϵ_i) and exhibit a nearly same pattern. Additionally, **Table (3)** displays some of the optical constant values ($\lambda = 550$ nm).

5. Conclusion

ZnTe thin films were effectively deposited using Physical Vapor Deposition in Vacuum, exhibiting uniform, smooth, and crack-free characteristics on glass substrates. Their structural qualities were confirmed through XRD, indicating a cubic crystal structure with preferred (111) orientation. AFM imaging revealed enhanced surface morphology and low RMS roughness as annealing temperature rose, with grain size increasing to 48.36 nm. The films demonstrated a direct transition electronic type, with the energy gap decreasing from 2.15 to 2.02 eV at higher annealing temperatures, making them suitable for solar cells and optoelectronic devices. Additionally, increased absorbency in the visible range was noted, along with a rise in the absorption and extinction coefficients.

Acknowledgment

We thank the Thin Film Lab., Department of Physics, College of Education for Pure Science /Ibn Al-Haitham, University of Baghdad.

Conflict of Interest

The authors declare that they have no conflicts of interest

Funding

We hereby confirm that all the Figures and Tables in the manuscript are ours

Ethical Clearance

The project was approved by the local ethical committee at the University of Baghdad.

References

1. Sarmad MA, Alia AA, Shehab. Effect of Cu doping on the electrical properties of ZnTe by Vacuum Thermal Evaporation. Ibn Haitham J Pure Appl Sci. 2018;31(3):20–25. <https://doi.org/10.30526/31.3.2023>
2. Chamola P, Mittal P. Zinc telluride material properties for solar cell application: Absorber layer. Main Group Chemistry. 2024;23(3):251–70. <https://doi.org/10.3233/mgc-230087>

3. Rajpal S, Kumar SR. Annealing temperature dependent structural and optical properties of nanocrystalline ZnTe thin films developed by electrodeposition technique. *Solid State Sci.* 2020;108:106424. <https://www.sciencedirect.com/science/article/abs/pii/S1293255820312966>
4. Bao X, Xue J, Yang X, Liu J, Yang H, Tang Z. Preparation and optimization of all-inorganic CdSe/ZnTe solar cells. *SSRN.* 2023. <https://ssrn.com/abstract=4717572>
5. Isik M, Gullu HH, Parlak M, Gasanly NM. Synthesis and temperature-tuned band gap characteristics of magnetron sputtered ZnTe thin films. *Physica B Condens Matter.* 2020;582:411968. <https://doi.org/10.1016/j.physb.2019.411968>
6. Panaitescu AM, Antohe I, Răduță AM, Iftimie S, Antohe Ș, Mihăilescu CN and Antohe V.A, Morphological, optical, and electrical properties of RF-sputtered zinc telluride thin films for electronic and optoelectronic applications. *AIP Adv.* 2022;12(11):111699. <https://doi.org/10.1063/5.0116999>
7. Kosasih FU, Erdenebileg E, Mathews N, Mhaisalkar SG, Bruno A. Thermal evaporation and hybrid deposition of perovskite solar cells and mini-modules. *Joule.* 2022;6:2692–734. <https://doi.org/10.1016/j.joule.2022.11.004>
8. Bushra H. Hussein and Hanan Hassun, Comparative Study for Optoelectronic Properties of Zn (Te, Se) Solar Cells. *NeuroQuantology.* 2020;18(5):77-82. <https://doi:10.14704/nq.2020.18.5.NQ20171>
9. Deng X, Zhao Q, Zhang H, Zhang F, Shen H. Bright and efficient green ZnSeTe-based quantum-dot light-emitting diodes with EQE exceeding 20%. *Sci Bull.* 2025;70(10):1619–26. <https://doi.org/10.1016/j.scib.2025.02.042>
10. Athab RH, Hussein BH. Fabrication and investigation of zinc telluride thin films. *Chalcogenide Lett.* 2023;20(7):477–85. <https://doi.org/10.15251/cl.2023.207.477>
11. Shiddiquee SN, Nushin S, Mondal BK, Abir TA, Rahman MM, Hossain M. Thiol-amine co-solvents aided direct synthesis of ZnTe thin films by spin coating for low cost optoelectronic applications. *arXiv.* 2024;2403:100458. <https://doi.org/10.1016/j.nxmate.2024.100458>
12. AlMaiyaly BH, Hussein BH, Shaban AH. Fabrication and characterization study of ZnTe/n-Si heterojunction solar cell application. *IOP Conf Ser: J Phys Conf Ser.* 2018;1003:012084. <https://doi.org/10.1088/1742-6596/1003/1/012084>
13. Hossain MI, Siddiquee K, Islam O, Gafur MA, Qadir MR, Ahmed NA. Characterization of electrodeposited ZnTe thin films. *J Opt.* 2019;48:295–301. <https://doi.org/10.1007/s12596-019-00550-0>
14. Athab RH, Hussein BH. Studying the effect of copper on the p-ZnTe/n-AgCuInSe₂/p-Si for thin films solar cell applications. *Chalcogenide Lett.* 2023;20(2):91–100. https://chalcogen.ro/91_AthabRH.pdf
15. Rajpal S, Kumar SR. Thermoluminescent properties of nanocrystalline ZnTe thin films: Structural and morphological studies. *Physica B Condens Matter.* 2018;534:145. <https://doi.org/10.1016/j.physb.2018.01.046>
16. Maki SA, Hassun HK. Effect of aluminum on characterization of ZnTe/n-Si heterojunction photodetector. *IOP Conf Ser: J Phys Conf Ser.* 2018;1003:012085. <https://doi.org/10.1088/1742-6596/1003/1/012085>
17. Salih AA, Mohammed AH, Aneed SH, Hussein BH. Fabrication and optoelectronic properties of bismuth oxide thin films prepared by thermal evaporation. *Iraqi J Appl Phys.* 2024;20(2B):387–92. <https://doi.org/10.2025/z62csh60>
18. Hasan Ali M, Haque MD, Hossain F, Touhidul Islam AZM. Touhidul Islam, Synthesis and characterization of spin coated ZnTe thin films for improving the efficiency of ZnTe/ZnS solar cell using SCAPS-1D. *RSC Adv.*, 2025;15:7069–7077. <https://doi.10.1039/d5ra00417a>
19. Zarei R, Ehsani MH, Rezaghiolipour Dizaji H. An investigation on structural and optical properties of nanocolumnar ZnTe thin films grown by glancing angle technique. *Mater Res Express.* 2020;7:026419. <https://doi.org/10.1088/2053-1591/ab7691>
20. Salih AA. The structural and surface morphology properties of aluminum doped CdO thin films prepared by vacuum thermal evaporation technique. *Ibn AL-Haitham J Pure Appl Sci.* 2014. <https://www.researchgate.net/publication/284456533>
21. Hassun HK, Hussein BH, Al-Maiyaly BKH, Moussa YKH, Shaban AH, Jasim KA. Impact thickness on performance of higher quality ZnTe photodetectors. *AIP Conf Proc.* 2025;3322(1):020018. <https://doi.org/10.1063/5.0289998>
22. Al Ahmed SR, Ferdous J. Development of a novel CdTe/ZnS/ZnTe heterojunction thin-film solar cells: A numerical approach. *IOP SciNotes.* 2020;1(2):2–10. <https://doi.org/10.1088/2633-1357/aba1f7>

23. Hussein BH, Hassun H. Comparative study for optoelectronic properties of Zn(Te, Se) solar cells. *NeuroQuantology*. 2020;18(5):77–82. <https://doi.org/10.14704/nq.2020.18.5.NQ20171>
24. Abood AH, Ramizy A, Albiss BA. Photoresponsive analysis of zinc telluride broadband photodetector fabricated using pulsed laser deposition technique. *Iraqi J Appl Phys*. 2024;20(4):787–92. <https://ijap-iq.com/index.php/ijap/article/download/39/135/1463>
25. Manica D, Antohe VA, Moldovan A, Pascu R, Iftimie S, Ion L, Sucheai MP. Thickness effect on some physical properties of RF sputtered ZnTe thin films for potential photovoltaic applications. *Nanomaterials*. 2021;11(9):2286–97. <https://doi.org/10.3390/nano11092286>
26. Rathod KC, Sanadi KR, Kamble PD, Kamble GS, Gaur M, Garadkar KL. Growth mechanism, structural and photoelectrochemical study of zinc tellurium thin film. *Asian J Chem*. 2022;34:715–22. <https://doi.org/10.14233/ajchem.2022.23458>
27. Ali RM, Najim FA. Depending the structural and optical properties of ZnTe thin films on Cd doping by thermal evaporation. *Q J Phys Sci*. 2024;29(2). <https://qjps.researchcommons.org/home/vol29/iss2/5/>
28. Ochoa-Estrella FJ, Vera-Marquina A, Mejia I, Leal-Cruz AL, Pintor-Monroy MI, Quevedo-López M. *Journal of Materials Science: Materials*. 2018;29:20623–28.
29. Dimple Singh, Naresh Padha, Zakir Hussain, Zahoor Ahmed and Padma Dolma, Growth of nanostructured ZnTe thin films through annealing of the MSEL D-prepared stack of precursors for photonic applications, *Chemical Physics Impact*, 2025: 10: 100837-100846. <https://doi.org/10.1016/j.chphi.2025.100837>
30. Babatunde RA, Odunaike RK. Optical, electrical properties and surface morphology of thermal evaporated zinc telluride (ZnTe) thin films for photovoltaic applications. *J Eng Technol Appl Phys*. 2022;4(2). <https://doi.org/10.33093/jetap>